EVS25

Shenzhen, China, Nov 5-9, 2010

Design and Analysis of Hybrid Power Systems with Variable Inertia Flywheel

Hung-Kuo Su[1], Tyng Liu[2]

[1, 2]*Department of Mechanical Engineering, National Taiwan University,*
No. 1, Sec. 4, Roosevelt Road, Taipei, 10617 Taiwan (R.O.C)
[1]*Graduate Student, R97522609@ntu.edu.tw*
[2]*Associate Professor, tliu@ntu.edu.tw*

Abstract

The purpose of this study is to analyze and to design for the hybrid power systems with variable inertia flywheel while the hybrid power system consists of 1 power plant, 1 variable inertia flywheel which is used as the energy storage device, a planetary gear set, and a set of actuators. First, the kinematic and kinetic equations of the hybrid power system are developed in order to establish the relationships of the speed and torque of all elements, and the specific speed and torque of the output needed for the vehicle can be found by using the software “ADVISOR” in various operation modes. Then, with the prescribed mechanical brake energy recovery system model and a control model, a comprehensive analysis can be achieved. Finally, various driving modes, such as ECE, ECE+EUDC and New York Bus driving mode are investigated in order to demonstrate the characteristics of the hybrid power system. The numerical results show and conclude the effectiveness of the variable inertia flywheel, and the improvement on the efficiency of hybrid power systems. Copyright Form of EVS25.

Keywords: brake energy regeneration, hybrid power system, variable inertia flywheel

1 Introduction

The researches on hybrid electric vehicles (HEV) are becoming more important in recent years, because the advantages of HEV are the significant reduction in fuel consumption and low emissions. Today, the cost of state-of-the-art batteries suitable for vehicular application remains high, and the use of a motor–generator and battery to transmit and retrieve the mechanical energy needs complicate systems for energy conversions [1]. In the search for a simple and practical hybrid system, the usage of a flywheel to retrieve energy in a hybrid system could be a possible design concept.

The use of flywheels in hybrid vehicles has been proposed by many researchers [1-6]. Flybrid Systems Company, in 2009, proposed a hybrid flywheel system, connected with drive shaft on the power train by continuous variable transmission, and then connected with flywheel by a clutch [2]. Diego-Ayala used only a planetary gear set to connect the output with the flywheel [1] and R.M. van Drute used a planetary gear set and continuous variable transmission to connect with a flywheel [3-6]. In all these concepts, the inertia of the flywheel is constant. It is possible that if the variable inertia flywheel is used, the energy storage and retrieve might become more effective and efficient.

The purpose of this study is to investigate the effectiveness and improvement of using a variable inertia flywheel in the hybrid power system for either electric vehicles or traditional internal combustion engine vehicles.

1.1 Hybrid Power Systems

The motor and transmission are the general vehicle components. In the hybrid power system, a variable moment of inertia flywheel, a planetary gear set and a set of actuator are added on to the system, as shown in Figure 1, [1]. The angular velocity and torque of the system can be expressed as the following equations:

$$(N_{31}-1)\omega_{Out} = -\omega_{Ring} + N_{31}\omega_{fw} \,, \quad (1)$$

$$\tau_{Ring} : \tau_{fw} : \tau_{Out} = 1 : -N_{31} : (N_{31}-1) \,, \quad (2)$$

where N_{31} is $-N_3/N_1$ and N_3 is gear number of sun gear, and N_1 is gear number of ring gear. In the equations, there are three variables, either for the angular velocities, or for the torques. Which means two variables should be assigned, or so called, controlled, and the system is said to be a two degree-of-freedom system.

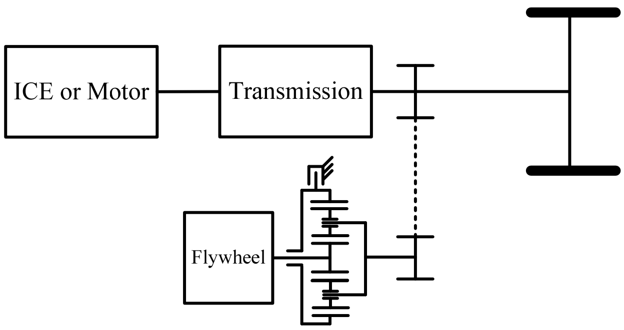

Figure 1: The Hybrid Power System Structure

In the system, there are actuators used to make the ring gear of planetary gear decelerate, so that the brake kinetic energy will be transferred to flywheel. When flywheel speed is high enough to drive the vehicle, the actuators will make the ring gear of planetary gear decelerate, and the flywheel kinetic energy will be transferred to the wheel to drive the vehicle. The operating logic is shown as Figure 2.

1.2 Equations of Hybrid Power Systems

The performance of the Hybrid Power System can be calculated by using equations (1) and (2). However, the losses at the gearbox should also be included by accounting for its efficiency η_{GB}. Depending on the direction of the energy flow, the torque loss T_{fw_loss} at the sun and the torque loss T_{Ring_loss} at the ring can be determined as the following.

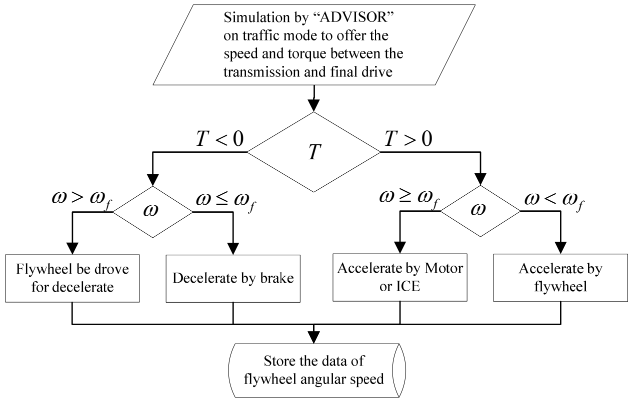

Figure 2: Operating logic for the System

1. If $T_{Out} > 0$ and $\omega_{Out} < (1-A)\,\omega_{fw}$, where $A = -1/(N_{31}-1)$, the vehicle will be accelerated by the flywheel. With respect to the require torque of vehicle, T_{Out}, the torque of the flywheel and the torque of the ring gear can be expressed as:

$$T_{fw} = -(1-A)T_{Out}\eta_{GB} \,, \quad (3)$$

$$T_{Ring} = -AT_{Out}\eta_{GB} \,. \quad (4)$$

The losses of torque in the transferring are:

$$T_{fw\_loss} = -(1-A)\tau_{Out}\left(\eta_{GB}-1\right), \quad (5)$$

$$T_{Ring\_loss} = -AT_{Out}\left(\eta_{GB}-1\right). \quad (6)$$

2. If $T_{Out} < 0$ and $\omega_{Out} > (1-A)\,\omega_{fw}$, the vehicle will be decelerated by the flywheel. The torque of the flywheel and the torque of the ring gear can be expressed as:

$$T_{fw} = -(1-A)T_{Out}/\eta_{GB} \,, \quad (7)$$

$$T_{Ring} = -AT_{Out}/\eta_{GB} \,. \quad (8)$$

The losses of the torques in the transferring are:

$$T_{fw\_loss} = -(1-A)T_{Out}\left(1/\eta_{GB}-1\right), \quad (9)$$

$$T_{Ring\_loss} = -AT_{Out}\left(1/\eta_{GB} - 1\right). \quad (10)$$

For a given torque T_{fw} acting on the flywheel, the change of the angular velocity of the flywheel can be determined by the rotational equation of motion, which is:

$$\Delta\omega_{fw} = \frac{\left(T_{fw} - T_{fw\_loss}\right)\Delta t}{I_{fw}}, \quad (11)$$

where $\triangle\omega_{fw}$, I_{fw}, and T_{fw_loss} are the change in speed, the inertia, and the torque losses of the flywheel respectively. The kinetic energy of the flywheel and the ring gear stored or released are:

$$E_{fw} = T_{fw}\omega_{fw}\Delta t, \quad (12)$$

$$E_{Ring} = T_{Ring}\omega_{Ring}\Delta t. \quad (13)$$

The operating logic for the hybrid power system combined with "ADVISOR" which is numerical simulation software [7]. They can be arranged to become a modular numerical simulation mode. The "ADVISOR" give the required torque and necessary angular velocity to the operating logic for the hybrid power system, and the operating logic for the hybrid power system will then determine the motor to be On or Off. The process is shown as in Figure 3.

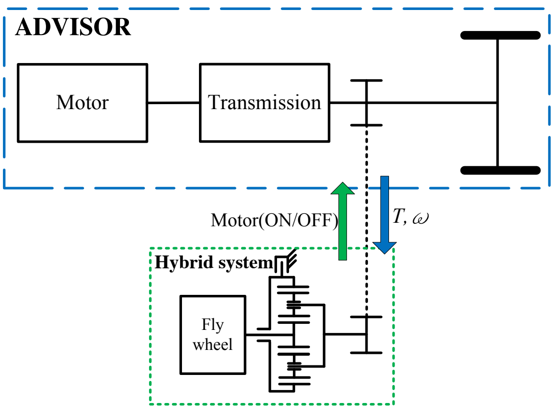

Figure 3: modular numerical simulation mode

1.3 Variable Inertia Flywheel Structure

In this study, the inertia of the flywheel can be various with respect to the speed of the flywheel [8]. The changing of the position of the lumped-mass will change the inertia of the flywheel as Figure 4.

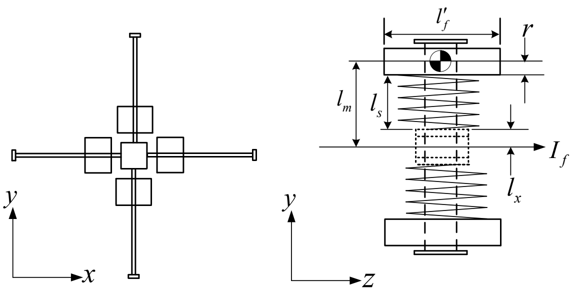

Figure 4: Variable Inertia Flywheel structure

To adjust or to change the inertia of the flywheel, can be in many different ways. It will certainly affect the ability of the flywheel in storing or releasing kinetic energy. In this case, the inertia of variable inertia flywheel is expressed by the following equation:

$$I_f = r\rho_f l_f'^2\left[\frac{2}{3}\left(l_f'^2 + 4r^2\right) + 8\left(\frac{\left(r + l_x\right)k_{spring}}{\left(k_{spring} - m\omega^2\right)}\right)^2\right] \quad (14)$$

The mass of variable inertia flywheel is expressed by the following equation:

$$m_f = 4\cdot\left(2r\rho_f l_f'^2\right). \quad (15)$$

After calculation, the stored energy of a variable inertia flywheel is shown as Figure 5.

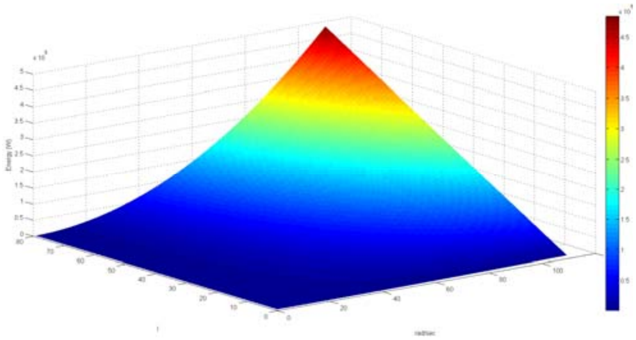

Figure 5: variable inertia flywheel of stored energy map

In Figure 5, the X-axis is the speed of the flywheel, the Y-axis is the inertia, and Z-axis shows how much energy could be restored. As shown, the relationship of the inertia and the changing of the inertia of the flywheel with the overall efficiency is implicit, and need some detailed numerical simulations to evaluate all design parameters and their interaction. Now if projection of Figure 5 is on X-Y flat and with a different function, which the inertia is varied with the angular velocity, is selected, the way of changing inertia of the flywheel is shown in Figure 6.

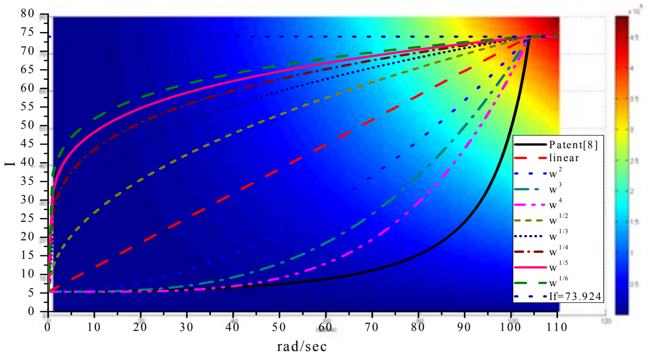

Figure 6: Different function of the flywheel on the energy map

1.4 Test Conditions

A 15,433 kg electric bus which the magnitudes of these weights, the specifications of test vehicle, the variable Inertia flywheel and battery are shown in 7.Appendix. The motor of 137(W) is shown as Figure 7. The X-axis is torque, the Y-axis is revolutions per minute (rpm), and Z-axis is the efficiency in transferring energy.

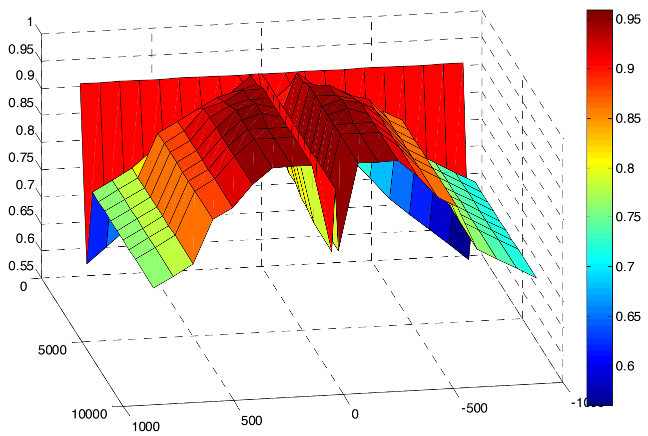

Figure 7: Motor characteristic

Whereas the flywheel's losses map, including bearing friction and wind resistance losses, was developed on the basis of experimental tests performed by Suzuki [9]. These values change dynamically as the simulation runs, whose main data is shown as Figure 8.

To assess the hybrid vehicle under city driving conditions, three widely accepted driving cycles were selected: the ECE cycle [10], the ECE+EUDC cycle[10] and New York bus cycle [11], whose main data are shown in Table 1 and the driving cycles are shown as Figure 9~11.

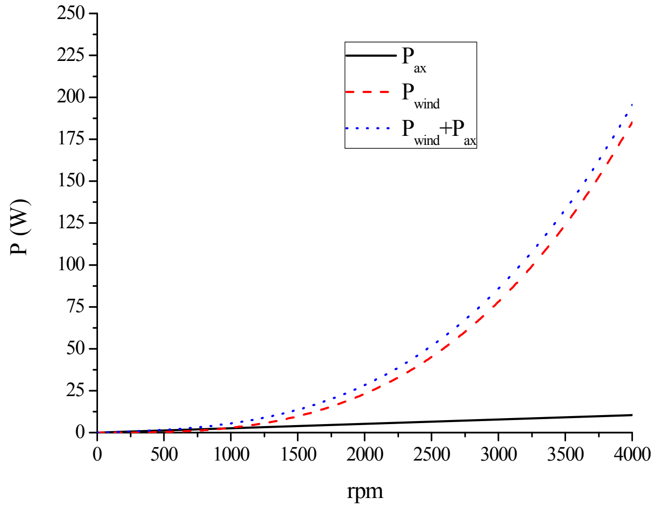

Figure 8: Energy losses at the flywheel

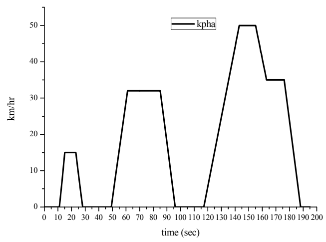

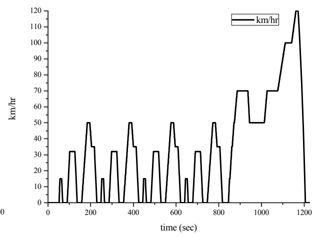

Fig. 9: ECE cycle[10] Fig. 10:ECE+EUDC cycle [10]

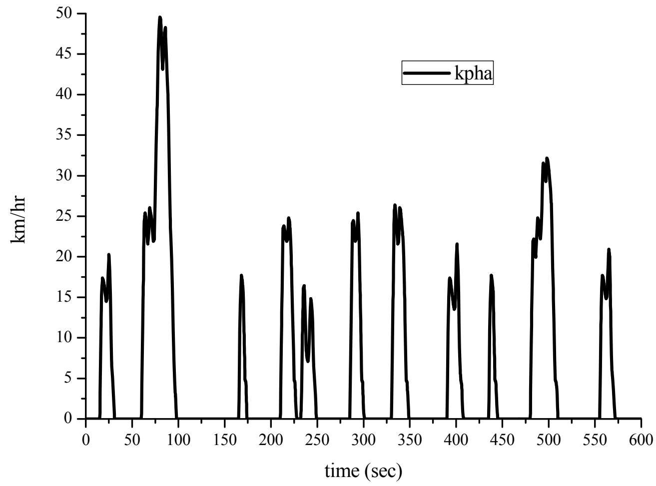

Figure 11: NewYork Bus cycle [11]

Table 1: Data of driving cycle

parameters	ECE cycle	ECE+EUDC cycle	NewYork bus cycle
Time	195 sec	1225 sec	600 sec
Distance	0.99 km	10.93 km	0.99 km
Idle time	64 sec	339 sec	404 sec
No. of stops	3 times	13 times	11 times
Max speed	49.55 km/hr	120 km/hr	49.57 km/hr
Average speed	18.26 km/hr	32.1 km/hr	5.93 km/hr
Max acceleration	1.06 m/sec^2	1.06 m/sec^2	2.77 m/sec^2
Max deceleration	−0.83 m/sec^2	−1.39 m/sec^2	−2.06 m/sec^2
Average acceleration	0.64 m/sec^2	0.54 m/sec^2	1.17 m/sec^2
Average deceleration	−0.75 m/sec^2	−0.79 m/sec^2	−0.67 m/sec^2

2 Comparisons of various driving modes

The SOC (State of Charge) of the vehicle before testing the driving mode is $SOC_{initial}$. When the vehicle finishes the driving mode, the SOC is $SOC_{remained}$, and the SOC used, is SOC_{used}. They are related as:

$$SOC_{used}=SOC_{initial}-SOC_{remained}\,. \quad (16)$$

For the comparison, the EI (Efficiency Improve) index is defined. Here we first define SOC_{basic} = SOC_{used} of a no-recharged EV after complete the driving test as the baseline of comparison. The EV index is expressed as:

$$EI=\left[\frac{(SOC_{basic}-SOC_{used})}{SOC_{used}}\right]\times 100\%\,. \quad (17)$$

The EI index is showing the improvement of the compared hybrid vehicle. Its physical meaning is that how farther, in percentage, the tested hybrid vehicle can go while using the same SOC as the no-recharged EV.

Here we set up A 15,433 kg electric bus of the hybrid power systems with fixed inertia flywheel, and simulate to run the ECE cycle for one time. We set the fixed inertia flywheel of I=24.1. For the planetary gear set, $A=0.89$, $N_{31}=-N_3/N_1=-0.1236=-11/89$, gear number of sun gear is 11, gear number of ring gear is 89 and gear number of planetary gear is 39.

We focus on 45sec to 100 sec for the acceleration and the deceleration, as shown in Figure 12. The red line is the driving mode whose unit is km/hr, and the angular speed of the planetary gear set with the reduction ratio is the black line. The green line is the angular velocity of the flywheel. The blue line is the angular velocity of the ring gear.

At 49.2 sec, the bus shall start to accelerate, and the flywheel and the ring gear will slow down. When the speed of flywheel and the speed of bus with the reduction ratio get very close, the actuator will then stop action, and the bus will be driven by original power source (here it is the motor) and so the flywheel is free spinning now.

When 85.2 sec, the bus shall decelerate, and the flywheel begins to accelerate and the ring gear begins slowly down. When the speed of flywheel and the speed of bus with the reduction ratio get very close, during the deceleration, again the actuator would stop action. Than the bus will be decelerated by its original brake system and flywheel will be free spinning again.

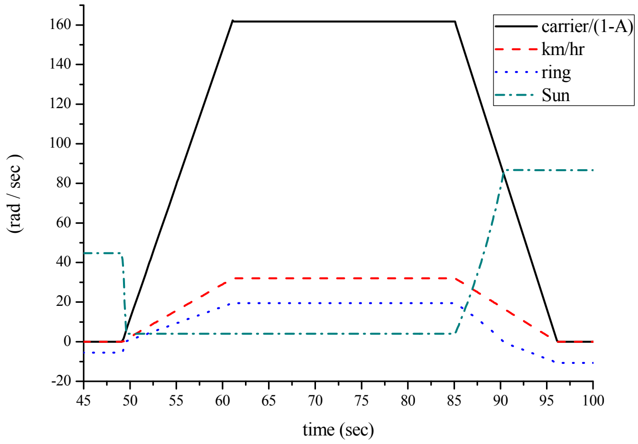

Figure 12: ECE cycle for each component in 45~100 sec

For the hybrid power systems with fixed inertia flywheel, adjusting the reduction ratio and the operation speed, which is range of operation of the flywheel while driving the vehicle, will clearly affect the $SOC_{remained}$. To compare the results of all variations, we have the simulation of running the ECE cycle for 5850 sec, and results are shown in Figure 13. The X-axis is the operation speed of the flywheel, the Y-axis is the reduction ratio of the planetary gear set, and the Z-axis is $SOC_{remained}$. We find the reduction ratio of the planetary gear set, 0.89 and operation speed, 11 rad/sec will give the most $SOC_{remained}$. These parameters will be set up for electric bus of the hybrid power systems with fixed inertia flywheel for further discussion.

Use the same way to search the better parameters for the hybrid power systems with variable inertia flywheel.

We find the set of parameters gives the most $SOC_{remained}$ is the inertia of the flywheel using the function $I(\omega)=\omega^{1/6}$, as shown in Table 2.

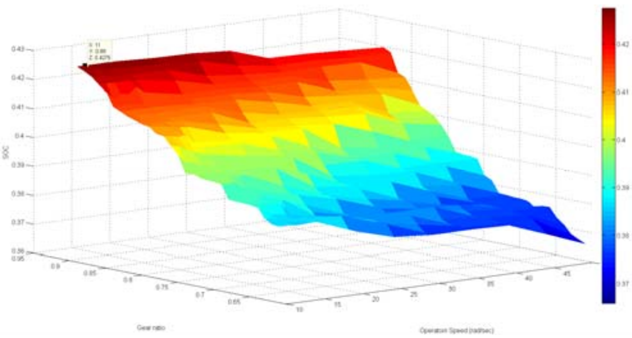

Figure 13: Optimization of parameters map for fixed inertia flywheel

Table 2 Optimization of parameters for variable inertia flywheel

	$SOC_{remained}$	SOC_{used}	EI %
Patent[8]	0.42347	0.57653	10.2569
Linear	0.45037	0.54963	15.6531
ω^2	0.44825	0.55175	15.2087
ω^3	0.44737	0.55263	15.0252
ω^4	0.44618	0.55382	14.7781
$\omega^{1/2}$	0.45202	0.54798	16.0013
$\omega^{1/3}$	0.45229	0.54771	16.0585
$\omega^{1/4}$	0.45244	0.54756	16.0903
$\omega^{1/5}$	0.45253	0.54747	16.1094
$\omega^{1/6}$	0.45261	0.54739	16.1263
I=73.924	0.45241	0.54759	16.0839
EV W/FW I=24.1	0.42746	0.57254	11.0253
EV W/RB	0.44236	0.55764	13.9924
EV	0.36433	0.63566	0

With the best parameters, we simulate the bus to run the New York bus cycle for 100 minutes, and results are shown as Figure 14. The green line is the hybrid power systems with variable inertia flywheel, whose $SOC_{remained}$ is the greater than the other hybrid vehicles. The blue line is the hybrid power systems with fixed inertia flywheel, whose $SOC_{remained}$ is also greater than the EV with regenerative brake, which is the red line.

Now we will simulate the hybrid power systems with a variable inertia flywheel to run the ECE cycle for 5850 sec, ECE+EUDC for 3675 sec and the New York bus cycle for 100 minutes and compare the results, as shown in Table 3.

There is an EI improvement, upto 33.7% for the EV with the variable inertia flywheel ($I = a + b\omega^{1/6}$). It is better than EV with fixed inertia flywheel (I = 24.1) and EV with brake electric energy regeneration.

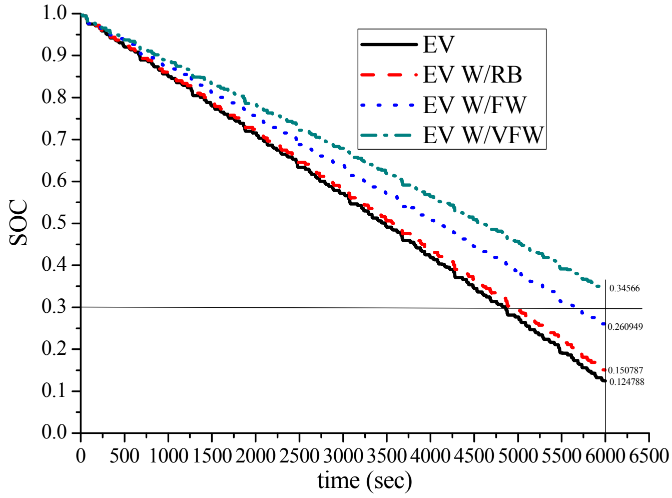

Figure 14: $SOC_{remained}$ of vehicles using NewYork bus cycle

Table 3: Simulation results

EI %	ECE	ECE +EUDC	New York bus Cycle
EV without energy regeneration	0	0	0
EV with brake electric energy regeneration	13.99	7.54	3.0615
EV with Flywheel (I = 24.1)	11.03	6.04	18.4238
EV with variable inertia Flywheel ($I = a + b\omega^{1/6}$)	16.13	9.03	33.7549

The increased EI is mainly because of the nature of the New York bus cycle. In the New York bus cycle, there are accelerations and decelerations 11 times in 10 minutes, and during 90% of the cycle time, the vehicle speed is lower than 20 km/h, and about 67% of the cycle time the bus is stalled. Since the electric machine of EV will operate in low efficiency when the vehicle is at low speed and demands high torque, the electric machine used in EV bus for braking energy recovery will not be very suitable. It only has 3% improvement, even less that in the case of ECE cycle.

For the New York bus cycle, when using the variable inertia flywheel ($I = a + b\omega^{1/6}$) to store and retrieve energy, the large amount of energy input and output can be coped with the vehicle speed, and provide better arrangement of the energy. While in low speed, the small inertia flywheel can be accelerated quickly to the operation speed and spinning into a large inertia flywheel, which is more suitable for kinetic energy storage and release. However, for the flywheel which is fixed inertia, the flywheel with large inertia will not speed up quick enough, and with small inertia just cannot store enough energy to drive the bus.

3 Conclusions

From our simulations, the results are all favored for the HEV with variable inertia flywheel. The improvement, EI index can be from 16.1% upto 33.8%, especially in case of New York bus cycle. Here are some summarized remarks.

1. Various types of hybrid power systems are investigated and compared numerically to evaluate the effectiveness of their energy recovery performance in different driving patterns.
2. On the energy recovery systems, the electric bus using variable inertia flywheel in the New York bus Cycle simulation can improve up to 33.8% efficiency better than the EV bus without energy regeneration, and also better than other hybrid power system evaluated in this study.
3. The hybrid power system with variable inertia flywheel is satiable for a heavy-vehicle in the stop- and-go with severe acceleration-and-deceleration operation. With the aid of the variable inertia flywheel, the motor, or the power plant, can be operated more efficiently and energy recovered is also increased with the help of the variable inertia flywheel if the range of operation, size, and the adjustment of the inertia of the flywheel have been selected and designed properly.

Acknowledgements

The support of Giant Lion Know-How Co. Ltd. to this research is gratefully appreciated, and the special thanks is to Mr. Tai-Her Yang, for his helpful and inspiring discussions during the course of this research.

References

[1] Diego-Ayala, U., Martinez-Gonzalez, P., McGlashan, N., *The mechanical hybrid vehicle: an investigation of a flywheel-based vehicular regenerative energy capture system*, Proceedings of the Institution of Mechanical Engineers part D- Journal of Automobile Engineering, vol. 222(2008), no. 11, pp.2087-2101.

[2] Flybrid Systems Company: http://www.flybridsystems.com/.

[3] Druten, R.M., *Transmission Design of The Zero Inertia Powertrain*, Ph.D. dissertation(2001), Tech. Univ. Eindhoven, Eindhoven, The Netherlands.

[4] Serrarens, F. A., and Veldpaus, F. E., *Control of A Flywheel Assisted Driveline with Continuously Variable Transmission, ASME Dynamic Systems*, Measurement and Control, Vol. 125(2003), no. 3, pp. 455-461.

[5] Shen, S., and Veldpaus. F. E., *Analysis and Control of a Flywheel Vehicular Powertrain,* IEEE Transaction on Control Systems Technology, Vol. 12(2004), no.5 pp.645-660.

[6] Shen, S., Vroemen, B., and Veldpaus. F. E., *IdleStop and Go: a way improve fuel economy,* Vehicle System Dynamics, Vol. 44(2006), no.6, pp.449-476.

[7] Markel, T., Brooker, A., Hendricks, T., Johnson, V., Kelly, K., Kramer, B., O'Keefe, M., Sprik, S., Wipke, K., *ADVISOR: a systems analysis tool for advanced vehicle modeling,* Journal of Power Sources, vol. 110(2002), no. 2, pp.255-266.

[8] Yang, Tai-Her, *Principle and structure of actively driving or centrifugal linear following dynamic flywheel effect*, US Patent (1993) No. 5,269,197.

[9] SuZuki, Y., Koyangi, A., Kobayashi, M., Shimada, R., *Novel applications of the flywheel energy storage system*, Renewable Energy, Vol. 30(2005), pp.2128-2143.

[10] EEC Directive 90/C81/01, *Emission test cycles for the certification of duty vehicles in Europe*, EEC emission cycles (1990).

[11] Michael P., *Emissions Results from Hybrid-Electric and Conventional Transit Buses in New York City*, West Virginia University (2000).

[12] Su, Hung-Kuo, *Design and Analysis of Hybrid Power Systems with Variable Inertia Flywheel*, Master Thesis(2010), National Taiwan University, Taipei , Taiwan.

Authors

Hung-Kuo Su
Room 508, College of Engineering building, No. 1, Sec. 4, Roosevelt Road, Taipei, 10617 Taiwan (R.O.C)
Tel: +886-926-282-232
Fax:+ 886-2-23631755
Email: R97522609@ntu.edu.tw
He received his M.S. in Mechanical Engineering from National Taiwan University, Taiwan, in 2010.

Tyng Liu
Room 630, College of Engineering building, No. 1, Sec. 4, Roosevelt Road, Taipei, 10617 Taiwan (R.O.C)
Tel: +886-2-3366-2709
Fax: +886-2-23631755
Email: tliu@ntu.edu.tw
He received his PhD in Mechanical Engineering from Rutgers University, U.S.A., in 1986. Dr. Liu is an Associate Professor of Department of Mechanical Engineering, National Taiwan University.

Appendix

Weight of the test vehicle

parameters	weight
Vehicle	12156 kg
Motor (137kw)	255 kg
Transmission (1 speed)	50 kg
Battery (Li ion)	1135 kg
passenger	1837 kg
Total	15433 kg

Specifications of the test vehicle

parameters	Value
g (gravity)	9.81 m/s^2
ρ (Air density)	1.23 kg/m^3
μ (road adhesion)	0.85
R_r(Rolling resistance)	0.01
Weight distribution (front : back)	0.635:0.365
C_D(coefficient of aerodynamic drag)	0.79
A_f(Forward projected area)	7.8965 m^2
h (Center of gravity height)	0.7747 m
L (Wheelbase)	7.4371 m
Wr (Wheel radius)	0.5 m
Iw(Wheel inertia)	20.52154
Gear box	One speed 1:1
Passengers weight	150/2.2046×27 =1837.068 kg (ref. SAE 931788)

Specifications of Variable Inertia Flywheel

parameters	Value
l_f	0.103 m
ρ_f	7900 kg/m^3
l'_f	0.1 m
R	0.159 m
l_x	0.05 m
k_{spring}	9×104 N/m
M	25.122 kg
I_f	5.32~73.924 (13.89times)
Total mass	100.673 kg

Specifications of the battery

parameters	Value
Temperature range	0 ~ 25 ~ 41 (℃)
Max Ampere for charge and discharge	5.943 ~ 7.035 ~ 7.405 (Ahr)
Efficiency of charge and discharge	0.968 ~ 0.99 ~ 0.992
Voltage range	11.7(V)~6(V)
Weight of one cell	1.13472 (kg)
Average heat capacity	795 (J/kgK)
Temperature of keeping	35 (℃)
Cooling of the surface	0.032 (m^2)
Air flow	0.07/12 (kg/s)
thickness of fin	0.001 (m)
Thermal coefficient	15 (W/m^2K)